Stereological assessment of the dorsal anterior cingulate cortex in schizophrenia: absence of changes in neuronal and glial densities

Malin Höistad[1,2], **Helmut Heinsen**[3], **Bridget Wicinski**[1], **Christoph Schmitz**[4], and **Patrick R. Hof**[1]

[1]Fishberg Department of Neuroscience and Friedman Brain Institute, Mount Sinai School of Medicine, New York, NY, USA

[2]Swedish Council on Health Technology Assessment, Stockholm, Sweden

[3]Department of Psychiatry, Morphological Brain Research Unit, University Würzburg, Germany

[4]Department of Anatomy, School of Medicine, Ludwig-Maximilians University, Münich, Germany

Abstract

Aims—The prefrontal and anterior cingulate cortices are implicated in schizophrenia, and many studies have assessed volume, cortical thickness, and neuronal densities or numbers in these regions. Available data however are rather conflicting and no clear cortical alteration pattern has been established. Changes in oligodendrocytes and white matter have been observed in schizophrenia, introducing a hypothesis about a myelin deficit as a key event in disease development.

Methods—We investigated the dorsal anterior cingulate cortex (dACC) in 13 males with schizophrenia and 13 age- and gender-matched controls. We assessed stereologically the dACC volume, neuronal and glial densities, total neuron and glial numbers, and glia/neuron (GNI) ratios in both layers II-III and V-VI.

Results—We observed no differences in neuronal or glial densities. No changes were observed in dACC cortical volume, total neuron numbers, and total glial numbers in schizophrenia. This contrasts with previous findings and suggests that the dACC may not undergo as severe changes in schizophrenia as is generally believed. However, we observed higher glial densities in layers V-VI than in layers II-III in both controls and patients with schizophrenia, pointing to possible layer-specific effects on oligodendrocyte distribution during development.

Conclusions—Using rigorous stereological methods, we demonstrate a seemingly normal cortical organization in an important neocortical area for schizophrenia, emphasizing the importance of such morphometric approaches in quantitative neuropathology. We discuss the significance of subregion- and layer-specific alterations in the development of schizophrenia, and the discrepancies between post-mortem histopathological studies and *in vivo* brain imaging findings in patients.

Keywords

dysmyelination; oligodendrocytes; white matter; morphology; cytoarchitecture; myelin

Correspondence: Dr Patrick R. Hof, Department of Neuroscience, Mount Sinai School of Medicine, Box 1065, One Gustave L. Levy Place, New York, NY 10029, USA. Tel: + 1-212-659-5904, Fax: + 1-212-849-2510 patrick.hof@mssm.edu.

None of the authors has any conflict of interest to declare in relation to this submission.

INTRODUCTION

White matter deficits and oligodendrocyte pathology have gained increasing interest in schizophrenia research, in light of findings that showed changes in expression levels of myelin and oligodendrocyte-related genes [1–3], and previous imaging findings showing alterations in the white matter [4, 12]. The myelin hypothesis in schizophrenia has been extensively reviewed in [13–18]. In the present study, we further investigate the role of a myelin deficit, in the context of possible neuropathology of the anterior cingulate cortex (ACC) in schizophrenia.

The ACC has been much studied in schizophrenia. It is known to play a role in the regulation of cognition, attention, emotions, and in social interactions. In the human brain, the ACC can be subdivided along its rostrocaudal and dorsoventral axes, through which there exist gradients in cytoarchitecture and topography in its afferent and efferent projections [19–22]. The ACC consists of areas 24 and 25 surrounding the genu of the corpus callosum. Some authors also include the paracingulate area 32 in the ACC. Cytoarchitecturally the ACC is complex and can be divided into distinct subregions [19, 21–23], and displays large individual variability and hemispheric asymmetry in the human brain [19]. The ACC receives multimodal sensory information from insular, temporal, and parietal association cortices, and emotional information from the amygdala and the orbitofrontal cortex [24–28]. It shows extensive connectivity with the dorsolateral prefrontal cortex. Specifically, the dorsal ACC (dACC, or supragenual part) is connected with the dorsolateral prefrontal and premotor areas, while the rostral ACC (rACC, or subgenual and pregenual parts) is connected with the amygdala and the orbitofrontal cortex [29]. These different connectivity patterns establish two functional ACC domains, a dorsal cognitive subdivision and a ventral affective subdivision, as demonstrated by imaging studies [30–32]. Based on its connections with other areas, the dACC (corresponding to subdivisions 24a'b' and c') is involved in attention to action, error detection, and motor functions [30], while the rostral ACC (corresponding to subdivisions 24abc, area 25 and the paracingulate area 32) is involved in the evaluation and regulation of emotion [33, 34].

Stereologicalal methods have been used to investigate the oligodendrocyte densities and distribution patterns in the dorsolateral prefrontal and anterior cingulate regions. Oligodendrocyte densities have previously been found to be decreased in schizophrenia in white and grey matter in area 9 [35], and in area 24 [36], but not in area 32 [36], or in the cingulum bundle [37]. Morphometric studies of neuron densities have been made in a limited number of cortical regions, and investigators have observed decreases in neuronal densities in area 24 [38], while increases have been found in areas 9 and 46 [39, 40]. However, using unbiased stereologicalal approaches, these findings have not been replicated. Moreover, brain imaging findings frequently reporting decreases in cortical or white matter volumes [41–45] are difficult to correlate to volume estimates from neurohistological methods. To investigate further the neuropathology of neurons and glia in schizophrenia in the ACC region, we studied the dACC using stereologicalal approaches.

MATERIALS AND METHODS

Subjects

This study was performed on the same post-mortem brains (both hemispheres) from 13 male patients with schizophrenia and from 13 age-matched male controls that were investigated in our previous studies on neuron numbers in subcortical regions [46], capillary length densities in the frontal cortex [47], and mean neuron spacing abnormalities in the neocortex [48].

All cases with schizophrenia had been patients either in German university hospitals or in German State psychiatric hospitals and full clinical records were available. All control cases had been patients either in German university hospitals or in German local district hospitals. Patients with schizophrenia and controls were similar in terms of ethnic background. In all of the cases, autopsy was performed after consent was obtained from a relative according to the laws of the Federal Republic of Germany. The use of autopsy cases for scientific investigations was approved by the relevant institutional review boards and ethics committees. Records from autopsy (including a summary of the medical history) were available for all patients with schizophrenia, and for all controls. All patients with schizophrenia met the diagnostic criteria of the Diagnostic Statistical Manual, DSM-IV [49] and International Statistical Classification of Diseases and Related Health Problems, ICD-10 [50]. All patients with schizophrenia were subjected to long-term treatment with typical neuroleptics. However, due to the fact that most of the patients were not hospitalized throughout the duration of their illness, the clinical records did not cover fully the entire medication histories and it was therefore not possible to calculate lifetime medication exposures. The clinical notes were assessed by two experienced clinical psychiatrists for clear evidence that the diagnosis of patients with schizophrenia was concordant with DSM-IV criteria for schizophrenia, and to ensure that the brains from the controls were free from psychopathology.

All pathologists involved in the autopsies were instructed by H.H. and adhered to identical handling and processing conditions of the brains. Brains were fixed by immersion in 4% formalin (one part 40% aqueous formaldehyde in nine parts H_2O) ranging from three months to ten years prior to histological processing as previously described [51]. The age of the patients, clinical diagnoses, illness duration, causes of death, the post-mortem interval and the fixation time are summarized in Table 1. The patients with schizophrenia did not differ from the controls with respect to mean age (two-tailed Student's t-test; $P = 0.946$), mean post-mortem interval ($P = 0.581$) and mean fixation time ($P = 0.089$). The mean age at onset of the patients with schizophrenia was 22.9 ± 1.5 years.

Exclusion criteria for both patients with schizophrenia and the controls comprised neurological problems that required intervention or interfered with cognitive assessment (e.g., stroke with aphasia), history of recurrent seizure disorder, history of severe head injury with loss of consciousness, history of other psychiatric illness, history of self-administered intoxication, and diabetes mellitus with free plasma glucose >200 mg/dl. After histological processing of the brains, each section was coded and verified for the absence of tumours, infarcts, heterotopias, signs of autolysis, staining artefacts and gliosis. In addition, from all the brains of the schizophrenic patients and controls older than 40 years, sections through the central portion of the entorhinal and transentorhinal cortex that were not stained with gallocyanin (see details below) were labelled with the Gallyas method to detect neurofibrillary changes [52]. Neurofibrillary tangles were very rarely detected in the transentorhinal and entorhinal cortex on Gallyas-stained sections, compatible with Braak's stage I [53].

Tissue processing

The brainstem with the cerebellum was separated from the forebrain at the level of the rostral pons, and the hemispheres were divided medio-sagittally. Both hemispheres were then cut into serial 600–700μm-thick coronal sections as previously described [51]. Briefly, the hemispheres were cryoprotected in a mixture of 2% glycerol-dimethylsulfoxide/ 4% formaldehyde/ 10–20% glycerol after carefully removing the meninges and the pial vessels, embedded in gelatin or agarose (15% gelatin or 3% agarose) hardened at 4°C over night creating a 5–10mm-thick mantle surrounding the brain, further hardened in 4% formaldehyde at 4°C for up to 3 days, deeply frozen at -60°C and serially sectioned using a

cryomicrotome (Jung, Nussloch, Germany). One brain (C7) was embedded in celloidin as recently described [54] and was cut into serial 440-500μm-thick coronal sections using a sliding microtome (Polycut, Cambridge Instruments, UK). From each hemisphere, every second or third section was stained with gallocyanin (a Nissl stain) as previously described [51]. Fixation and tissue processing were performed at the Morphological Brain Research Unit, University of Wuerzburg (Germany) under identical conditions for all brains (except for brain C7 that was embedded in celloidin instead of gelatin).

Stereological analyses

Stereological analyses were performed with a stereology workstation equipped with a Zeiss Axioplan II microscope (Carl Zeiss MicroImaging, Thornwood, NY, USA), Plan-Neofluar objectives 2.5x (N.A. = 0.075) and 40x (N.A. = 1.30), Fluar objectives 10x (N.A. = 0.5) and 20x (N.A. = 0.75), a Microfire CCD camera (Optronics, Goleta, CA, USA), a motorized stage (Ludl Electronics, Hawthorne, NY, USA), and stereology software (StereoInvestigator, Version 10, MBF Bioscience, Williston, VT, USA).

The left hemispheres were selected and the regions of interest were delineated at low magnification (using the 2.5x objective) according to established criteria in the literature [19]. The regions of interest (ROI) were layers II-III and layers V-VI of the dACC region, corresponding to Brodmann's area 24, subregions 24a', 24b' and 24c' as described by Vogt [19]. Grossly, the most anterior section started from the crossing of the corpus callosum, and extended approximately 2 cm posteriorly to the border with area 23. Every 6th section was sampled in a consistent and unbiased manner, generating a serial section series of 5–7 sections within our ROIs. Actual section thickness after histological processing was determined as described in [55].

The volumes of the dACC region (layers II-III and layers V-VI) were analyzed using the Cavalieri principle [56]. Briefly, the area of the delineated ROIs was multiplied by the serial section interval and the actual measured section thickness. Estimation population of total neuron and total glial cell (astrocytes and oligodendrocytes) numbers in layers II-III and layers V-VI separately was evaluated using the Optical Fractionator method, see [56]. Starting with a random section number, a systematic random sampling throughout the ROI was performed. Pilot experiments were conducted to select appropriate counting frames and grid sizes, generating approximately 500 counted objects (either neurons or glia) in a total series, consistently generating coefficient of errors (CE) <0.1, see [56]. Details of the final counting procedures are summarized in Table 2. Neurons were identified by their characteristic morphology with dark and recognizable nucleoli, a large soma with a distinct cell nucleus surrounded by fainter cytoplasm, and dendrites emerging from the soma. Glial cells were identified by their smaller size, lack of processes, and dark homogenous staining. Astrocytes are nearly indistinguishable from oligodendrocytes in gallocyanin-stained materials [51], and were pooled together as glial cells. The neuron and glial cell densities were calculated as the ratio of the total cell number (either neuron or glia) and the Cavalieri volume of the ROIs. The glia/neuron index (GNI) was calculated as the ratio of the glial cell density to the neuron density.

Statistical analysis

For both patients with schizophrenia and controls, means and standard error of the mean (SEM) were calculated for age at death, age at onset of illness, post-mortem interval (PMI), and fixation time (Table 1). Means and SEM were also calculated (separately for patients with schizophrenia and controls) for the analyzed variables, dACC volume, total neurons, total glia, neuron density, glial density and GNI (separately for layers II–III and V-VI). Comparisons between patients with schizophrenia and controls were performed using

generalized linear model multivariate analysis (MANOVA), with diagnosis as fixed factor and the following variables as covariates: post-mortem interval (PMI), fixation time, age of controls or adjusted illness duration (AID) of patients with schizophrenia (AID is calculated as individual age at death minus age at onset plus the mean age at onset of all patients with schizophrenia). Note that use of the actual individual illness duration of the patients with schizophrenia instead of the adjusted ones as covariate would have caused invalid results of the MANOVA model because there was no illness duration of the controls. The mean illness duration of the patients with schizophrenia was significantly different from the mean age of the controls (two-tailed Student's t-test; $p < 0.001$) whereas the mean adjusted illness duration was not ($p = 0.974$). For each investigated variable, the two investigated regions of interest (layers II-III and V-VI) were tested simultaneously. In all analyses an effect was considered statistically significant if its associated p-value was <0.05. Calculations were performed using SPSS (Version 18.0.1 for Mac, PASW, Chicago, IL, USA). Graphical analysis was done with GraphPad Prism (Version 4 for Macintosh; GraphPad Software, La Jolla, CA, USA).

Photography

Photomicrographs of full brain sections were scanned at high resolution (600 dpi) using an Epson Perfection 2450 Photo scanner (Figure 2A). Photomicrographs of magnified regions were produced by digital photography using the stereology workstation with the StereoInvestigator software described above. Figures 2B and 3CD were generated using the Virtual Slide module, using either a 2.5x objective and a grid size of approximately 5x6 (Figure 2B), or a 10x objective and a grid size of 1x4 (Figure 3CD), grid size adjusted to the size of the area acquired. Figure 3AB was generated using the Deep Focus module with the 40x objective, acquiring images every 3–5μm through a section thickness of 20–30μm. All editing was performed using Adobe Photoshop CS4.

RESULTS

The region of interest

The region of the dACC used in our study encompassed the areas 24a'b'c', as delineated by Vogt and coworkers [19, 30], corresponding functionally to the cognitive subdivision of the ACC, as discussed by Bush et al. [31] (Figure 1). A representative coronal section through the dACC is shown in Figure 2. The investigated ROI extended from the rostralmost to the caudalmost levels of areas 24a', b', and c' (supplementary Figures 1–2). The ROI was also subdivided into superficial (layers II-III) and deep (layers V-VI) cortical layers because of known differences in cortical layer development and connectivity patterns [57]. The cytoarchitecture and the cellular features of the representative area 24b' is shown in Figure 3 (and supplementary Figure 3).

In human post-mortem Nissl-stained materials, oligodendrocytes may be difficult to distinguish reliably from astrocytes. However, it is known that astrocytosis (which is indicative of glial scarring and a gliotic reaction) is not present in schizophrenia [58], thus changes in glial cell numbers would suggest underlying changes in oligodendrocyte numbers. For histological analyses, no histochemical or immunohistochemical marker for specific for oligodendrocytes is sufficiently specific and reliable for quantification purposes on human postmortem tissue. As a consequence, in our Nissl-stained materials, we counted astrocytes and oligodendrocytes together as glial cells.

Observations in controls versus patients with schizophrenia

In the dorsal anterior cingulate region, we analyzed the dACC volume, the estimated population of total number of neurons, the estimated population of total number of glial

cells, the estimated neuron density, the estimated glial cell density, and the glia/neuron index (GNI), in layers II-III and layers V-VI of area 24a'b'c'. These variables were analyzed between groups (controls versus patients with schizophrenia) and against age and adjusted illness duration.

Using rigorous anatomical and stereological criteria, we found no differences between groups in either cortical volume, total neuron numbers, or total number of glial cells in the dACC (supplementary Figure 4). Similarly, we found no differences between groups in neuron density, glial density, or GNI values (Figure 4), as well as between groups when adjusting for illness duration, showing (not shown). These findings of an apparent intact dACC cytoarchitecture in schizophrenia stand in contrast to other observations of decreases as well as increases in neuronal densities in the cingulate or prefrontal cortex in patients with schizophrenia (see Discussion). Glial cell densities appeared to decrease with age and illness duration in both superficial and deep layers. However, as white matter volume generates an inverse U-shaped developmental pattern in healthy patients [59], regression analysis was not used to assess this apparent decrease (see Discussion).

Observations in superficial versus deeper cortical layers

In contrast to the lack of differences between groups, we found anticipated differences between cortical layers in both patients with schizophrenia and in controls (Figure 4). Overall, the neuron densities were higher in superficial layers, whereas the glial densities were higher in the deep layers. This was also reflected in the calculation of the glia/neuron ratios, the GNI in layers II-III was approximately 1.5 in both groups, and the GNI in layers V-VI was approximately 2.3 in both groups. We found differences in the superficial layers versus the deep layers in glial densities in the dACC, in both controls and patients with schizophrenia, reflecting that there were more glial cells in the deep layers.

DISCUSSION

Using rigorous anatomical and stereological criteria, we observed no changes in neuronal or glial cell densities in the dACC in patients with schizophrenia compared to controls from a cohort of age- and gender-matched subjects, spanning from 20 to70 years of age. Neither did we detect any changes in the volume, total neuron numbers, or total glial cell numbers in the dACC between patients with schizophrenia and controls. These findings do not support previous observations of apparent changes in neuron densities in prefrontal and cingulate regions in patients with schizophrenia. We did however find expected differences between superficial and deep layers in both neuron and glial cell densities, as well as the GNI, in the dACC in both controls and patients with schizophrenia. These observations can be attributed the importance of subregion- and layer- specificity when addressing neuropathological changes in schizophrenia. Differences in histopathological changes in post-mortem human tissue may reflect several methodological and technical differences (such as sample size, age-matched cases, left and right hemispheres, stereological versus two-dimensional analyses, section thickness, staining procedures, regional delineation, etc.). The present results emphasize the necessity to provide meticulously detailed methodological and analytical information in quantitative neuropathological studies.

Previous morphological data on cortical thickness and imaging data on regional volumes have suggested that different areas in schizophrenia may have a reduced volume [41, 44, 45, 60–63]. Despite the abundance of imaging data suggesting reduced volume of various cortical regions, these findings have been difficult to correlate with post-mortem histopathological data. Both subregion delineation as well as analytical differences between imaging and histopathological data may lie behind these difficulties. When investigating particular subregions of the anterior cingulate and prefrontal cortex, for example, Koo and

colleagues found volume differences in the subgenual and rostral ACC, but no volume differences in the dorsal ACC or in the posterior cingulate cortex [45]. A study by Narr and colleagues [43] found decreases in ACC thickness in women, whereas in men only slight decreases in dACC thickness in the right hemisphere were observed, with an overall increase in prefrontal cortical thickness. In histological materials, the reduction in brain volume in select areas has primarily been attributed to a reduction in neuronal size and in reduced neuropil, rather than a loss of neurons [64, 65]. Others have found indications of a decreased cortical thickness and smaller pyramidal soma size in area 24abc as well as in area 25 in schizophrenia, but with no changes in neuronal densities [66].

Studies on neuronal densities in the prefrontal cortex and the anterior cingulate cortex have led to inconclusive outcomes because rigorous stereological approaches have not been employed, different Brodmann areas have been pooled, or generalized theories have been presented from the results of only a few cortical regions. For these reasons, some authors find no changes in neuronal densities in schizophrenia, some find decreases in neuronal density, while others found increases in neuronal density. For methodological purposes in quantitative neuroanatomy, we discuss some examples of these inconclusive findings below.

Pakkenberg and coworkers employed stereology but found no changes in neuronal densities, yet these studies pooled several Brodmann areas from the prefrontal and cingulate cortex [67, 68]. In contrast, Stark and colleagues found no differences in neuronal densities in area 24 or 32 [36], and Bouras and coworkers found no differences in neuronal densities in area 24abc [66]. Benes and coworkers employed a 2D counting approach and found lower densities of neurons in the cingulate cortex while subregions were not specified [69, 70]. These reductions in neuron densities in the cingulate have not been replicated by others using stereological methods. Selemon and coworkers employed stereology and found higher neuronal densities in the prefrontal cortex, yet mainly focused on area 9 and 46 [39, 40]. They also found smaller soma sizes [71] and smaller frontal grey matter volume [60] and extrapolated these results to a generalized view of changes in the prefrontal cortex in schizophrenia [64]. In the ACC, Chana and colleagues also found increased neuronal densities and smaller soma sizes using stereologicalal methods [72]. Despite these discrepancies, these findings have supported the altered circuitry hypothesis of schizophrenia [64, 73]. However, the difficulty in comparing and evaluating these reports remains, as they contain methodological limitations that may have had influence the outcome.

Not as many studies have investigated glial density changes in schizophrenia. This may be due to the fact that there were apparently no astrogliotic changes occurring in schizophrenia [58], and the influence of potential oligodendrocyte changes was perhaps overlooked. In the prefrontal and cingulate regions, Hof and colleagues found decreased oligodendrocyte densities in area 9 [35], and Stark and coworkers found decreased oligodendocyte densities in area 24 but not in area 32 in schizophrenia [36]. In comparison, Segal and coworkers found no differences in oligodendrocytes densities in the cingulum bundle [37]. Reductions in glial densities have also been found in the subgenual anterior cingulate cortex in depression [74, 75]. These observations have previously suggested that changes in oligodendrocyte numbers may be indicative of aberrant wiring and conduction abnormalities in schizophrenia.

In assessments of neuropathological changes in cortical and subcortical architecture and histology, crucial components are to specify the region and subregions studied, since subtle changes may be present within one region [19,30, 31, 76]. For example, using the same cases as in this study, Kreczmanski et al. [46] found reduced volume and total neuron numbers, but not densities, in the putamen and lateral nucleus of the amygdala, but not in

other striatal or amygdala subregions. Within the ACC, the pregenual and subgenual regions have been shown to be relevant to emotional functions [77] and are strongly connected with the amygdala [78], and have primarily been implicated in depression [34, 79]. However the rACC has mainly been studied with imaging, as reliable morphometric or stereological investigations of the pregenual cortex are notoriously difficult in view of its curved morphology. Lastly, layer specificity in schizophrenia studies is particularly important considering that schizophrenia is also considered to be a neurodevelopmental disorder [86, 87, 88]. In this context, it is noteworthy that deep layers myelinate before superficial layers during development [80]. This may be the reason for higher numbers of oligodendrocytes in the deep layers, as found in this study. Any aberrations in cortical layering may be of substantial importance for the development of schizophrenia.

The theories on the aetiology and psychopathology of schizophrenia are multifaceted, from neurochemical to wiring and development. The fact that a myelination deficit potentially represents a substrate for the clinical symptoms seen in patients with schizophrenia merits to be reviewed in the context of developmental aberrations [81, 82] and altered cortical circuitry [65, 75, 83–86]. The myelin theory on schizophrenia originated from the finding of myelin pathology and downregulation of the expression of myelin-related genes in schizophrenia [1]. Myelin and oligodendrocyte integrity are required for adequate functioning of neurons and hence of circuitry. It has been shown that both white matter volume and grey matter volume changes during development and aging [59]. Sowell and coworkers found that the white matter development followed and inverted U-pattern, with white matter volume increasing until midlife and then declining, whereas the grey matter volume progressively decreases with age [59]. Therefore, a myelination deficit in schizophrenia, which has gained much support in recent years from white matter architecture and tractography imaging studies [85, 87–90], may be directly linked to both the theories of development and circuitry.

Our results, however, suggest that any neuropathological and neurohistological changes are highly region- and layer-specific. Myelin changes previously observed may perhaps be specifically localized to other areas of the prefrontal cortex, such as area 9 [35]. This is an intriguing outcome that points to fact that the dACC may not undergo as severe changes in its cellular makeup in schizophrenia as has been generally believed, and stresses the need for further detailed postmortem investigations, at the level of identified and specific domains of grey and white matter.

Supplementary Material

Refer to Web version on PubMed Central for supplementary material.

Acknowledgments

REFERENCES

1. Hakak Y, Walker JR, Li C, Wong WH, Davis KL, Buxbaum JD, Haroutunian V, Fienberg AA. Genome-wide expression analysis reveals dysregulation of myelination-related genes in chronic schizophrenia. Proc Natl Acad Sci U S A. 2001; 98:4746–4751. [PubMed: 11296301]

2. Tkachev D, Mimmack ML, Ryan MM, Wayland M, Freeman T, Jones PB, Starkey M, Webster MJ, Yolken RH, Bahn S. Oligodendrocyte dysfunction in schizophrenia and bipolar disorder. Lancet. 2003; 362:798–805. [PubMed: 13678875]

3. Dracheva S, Davis KL, Chin B, Woo DA, Schmeidler J, Haroutunian V. Myelin-associated mRNA and protein expression deficits in the anterior cingulate cortex and hippocampus in elderly schizophrenia patients. Neurobiol Dis. 2006; 21:531–540. [PubMed: 16213148]

4. Buchsbaum MS, Friedman J, Buchsbaum BR, Chu KW, Hazlett EA, Newmark R, Schneiderman JS, Torosjan Y, Tang C, Hof PR, Stewart D, Davis KL, Gorman J. Diffusion tensor imaging in schizophrenia. Biol Psychiatry. 2006; 60:1181–1187. [PubMed: 16893533]

5. Buchsbaum MS, Tang CY, Peled S, Gudbjartsson H, Lu D, Hazlett EA, Downhill J, Haznedar M, Fallon JH, Atlas SW. MRI white matter diffusion anisotropy and PET metabolic rate in schizophrenia. NeuroReport. 1998; 9:425–430. [PubMed: 9512384]

6. Lim KO, Hedehus M, Moseley M, de Crespigny A, Sullivan EV, Pfefferbaum A. Compromised white matter tract integrity in schizophrenia inferred from diffusion tensor imaging. Arch Gen Psychiatry. 1999; 56:367–374. [PubMed: 10197834]

7. Foong J, Maier M, Barker GJ, Brocklehurst S, Miller DH, Ron MA. In vivo investigation of white matter pathology in schizophrenia with magnetisation transfer imaging. J Neurol Neurosurg Psychiatry. 2000; 68:70–74. [PubMed: 10601405]

8. Foong J, Symms MR, Barker GJ, Maier M, Woermann FG, Miller DH, Ron MA. Neuropathological abnormalities in schizophrenia: evidence from magnetization transfer imaging. Brain. 2001; 124:882–892. [PubMed: 11335691]

9. Kubicki M, McCarley R, Westin CF, Park HJ, Maier S, Kikinis R, Jolesz FA, Shenton ME. A review of diffusion tensor imaging studies in schizophrenia. J Psychiatr Res. 2007; 41:15–30. [PubMed: 16023676]

10. Kubicki M, Park H, Westin CF, Nestor PG, Mulkern RV, Maier SE, Niznikiewicz M, Connor EE, Levitt JJ, Frumin M, Kikinis R, Jolesz FA, McCarley RW, Shenton ME. DTI and MTR abnormalities in schizophrenia: analysis of white matter integrity. Neuroimage. 2005; 26:1109–1118. [PubMed: 15878290]

11. Kubicki M, Westin CF, Nestor PG, Wible CG, Frumin M, Maier SE, Kikinis R, Jolesz FA, McCarley RW, Shenton ME. Cingulate fasciculus integrity disruption in schizophrenia: a magnetic resonance diffusion tensor imaging study. Biol Psychiatry. 2003; 54:1171–1180. [PubMed: 14643084]

12. Sun Z, Wang F, Cui L, Breeze J, Du X, Wang X, Cong Z, Zhang H, Li B, Hong N, Zhang D. Abnormal anterior cingulum in patients with schizophrenia: a diffusion tensor imaging study. NeuroReport. 2003; 14:1833–1836. [PubMed: 14534430]

13. Davis KL, Stewart DG, Friedman JI, Buchsbaum M, Harvey PD, Hof PR, Buxbaum J, Haroutunian V. White matter changes in schizophrenia: evidence for myelin-related dysfunction. Arch Gen Psychiatry. 2003; 60:443–456. [PubMed: 12742865]

14. Walterfang M, Wood SJ, Velakoulis D, Pantelis C. Neuropathological, neurogenetic and neuroimaging evidence for white matter pathology in schizophrenia. Neurosci Biobehav Rev. 2006; 30:918–948. [PubMed: 16580728]

15. Dwork AJ, Mancevski B, Rosoklija G. White matter and cognitive function in schizophrenia. Int J Neuropsychopharmacol. 2007; 10:513–536. [PubMed: 17313699]

16. Hoistad M, Segal D, Takahashi N, Sakurai T, Buxbaum JD, Hof PR. Linking white and grey matter in schizophrenia: oligodendrocyte and neuron pathology in the prefrontal cortex. Front Neuroanat. 2009; 3:9. [PubMed: 19636386]

17. Karoutzou G, Emrich HM, Dietrich DE. The myelin-pathogenesis puzzle in schizophrenia: a literature review. Mol Psychiatry. 2008; 13:245–260. [PubMed: 17925796]

18. Segal D, Koschnick JR, Slegers LH, Hof PR. Oligodendrocyte pathophysiology: a new view of schizophrenia. Int J Neuropsychopharmacol. 2007; 10:503–511. [PubMed: 17291369]

19. Vogt BA, Nimchinsky EA, Vogt LJ, Hof PR. Human cingulate cortex: surface features, flat maps, and cytoarchitecture. J Comp Neurol. 1995; 359:490–506. [PubMed: 7499543]

20. Öngür D, Ferry AT, Price JL. Architectonic subdivision of the human orbital and medial prefrontal cortex. J Comp Neurol. 2003; 460:425–449. [PubMed: 12692859]

21. Gittins R, Harrison PJ. A quantitative morphometric study of the human anterior cingulate cortex. Brain Res. 2004; 1013:212–222. [PubMed: 15193531]

22. Palomero-Gallagher N, Mohlberg H, Zilles K, Vogt B. Cytology and receptor architecture of human anterior cingulate cortex. J Comp Neurol. 2008; 508:906–926. [PubMed: 18404667]

23. Vogt, BA. Structural organization of cingulate cortex: Areas, neurons, and somatodendritic transmitter receptors. In: Vogt, BA., editor. Neurobiology of Cingulate Cortex and Limbic Thalamus. Boston: Birkhäuser; 1993. p. 19-70.

24. Jones EG, Powell TP. An anatomical study of converging sensory pathways within the cerebral cortex of the monkey. Brain. 1970; 93:793–820. [PubMed: 4992433]

25. Vogt BA, Pandya DN. Cingulate cortex of the rhesus monkey: II. Cortical afferents. J Comp Neurol. 1987; 262:271–289. [PubMed: 3624555]

26. Vogt BA, Pandya DN, Rosene DL. Cingulate cortex of the rhesus monkey: I. Cytoarchitecture and thalamic afferents. J Comp Neurol. 1987; 262:256–270. [PubMed: 3624554]

27. Van Hoesen, GW.; Morecraft, RJ.; Vogt, BA. Connections of the monkey cingulate cortex. In. In: Vogt, BA.; Gabriel, M., editors. Neurobiology of Cingulate Cortex and Limbic Thalamus. Boston: Birkhauser; 1993. p. 249-284.

28. Beckmann M, Johansen-Berg H, Rushworth MF. Connectivity-based parcellation of human cingulate cortex and its relation to functional specialization. J Neurosci. 2009; 29:1175–1190. [PubMed: 19176826]

29. Barbas H, Pandya DN. Architecture and intrinsic connections of the prefrontal cortex in the rhesus monkey. J Comp Neurol. 1989; 286:353–375. [PubMed: 2768563]

30. Vogt BA, Finch DM, Olson CR. Functional heterogeneity in cingulate cortex: the anterior executive and posterior evaluative regions. Cereb Cortex. 1992; 2:435–443. [PubMed: 1477524]

31. Bush G, Luu P, Posner MI. Cognitive and emotional influences in anterior cingulate cortex. Trends Cogn Sci. 2000; 4:215–222. [PubMed: 10827444]

32. Mohanty A, Engels AS, Herrington JD, Heller W, Ho MH, Banich MT, Webb AG, Warren SL, Miller GA. Differential engagement of anterior cingulate cortex subdivisions for cognitive and emotional function. Psychophysiology. 2007; 44:343–351. [PubMed: 17433093]

33. Etkin A, Egner T, Kalisch R. Emotional processing in anterior cingulate and medial prefrontal cortex. Trends Cogn Sci. 2011; 15:85–93. [PubMed: 21167765]

34. Beauregard M, Levesque J, Bourgouin P. Neural correlates of conscious self-regulation of emotion. J Neurosci. 2001; 21:RC165. [PubMed: 11549754]

35. Hof PR, Haroutunian V, Friedrich VL Jr, Byne W, Buitron C, Perl DP, Davis KL. Loss and altered spatial distribution of oligodendrocytes in the superior frontal gyrus in schizophrenia. Biol Psychiatry. 2003; 53:1075–1085. [PubMed: 12814859]

36. Stark AK, Uylings HB, Sanz-Arigita E, Pakkenberg B. Glial cell loss in the anterior cingulate cortex, a subregion of the prefrontal cortex, in subjects with schizophrenia. Am J Psychiatry. 2004; 161:882–888. [PubMed: 15121654]

37. Segal D, Schmitz C, Hof PR. Spatial distribution and density of oligodendrocytes in the cingulum bundle are unaltered in schizophrenia. Acta Neuropathol. 2009; 117:385–394. [PubMed: 18438678]

38. Benes FM. Evidence for neurodevelopment disturbances in anterior cingulate cortex of postmortem schizophrenic brain. Schizophr Res. 1991; 5:187–188. [PubMed: 1760386]

39. Selemon LD, Rajkowska G, Goldman-Rakic PS. Abnormally high neuronal density in the schizophrenic cortex. A morphometric analysis of prefrontal area 9 and occipital area 17. Arch Gen Psychiatry. 1995; 52:805–818. discussion 19-20. [PubMed: 7575100]

40. Selemon LD, Rajkowska G, Goldman-Rakic PS. Elevated neuronal density in prefrontal area 46 in brains from schizophrenic patients: application of a three-dimensional, stereologic counting method. J Comp Neurol. 1998; 392:402–412. [PubMed: 9511926]

41. Andreasen N, Nasrallah HA, Dunn V, Olson SC, Grove WM, Ehrhardt JC, Coffman JA, Crossett JH. Structural abnormalities in the frontal system in schizophrenia. A magnetic resonance imaging study. Arch Gen Psychiatry. 1986; 43:136–144. [PubMed: 3947208]

42. Nesvag R, Lawyer G, Varnas K, Fjell AM, Walhovd KB, Frigessi A, Jonsson EG, Agartz I. Regional thinning of the cerebral cortex in schizophrenia: effects of diagnosis, age and antipsychotic medication. Schizophr Res. 2008; 98:16–28. [PubMed: 17933495]

43. Narr KL, Bilder RM, Toga AW, Woods RP, Rex DE, Szeszko PR, Robinson D, Sevy S, Gunduz-Bruce H, Wang YP, DeLuca H, Thompson PM. Mapping cortical thickness and gray matter concentration in first episode schizophrenia. Cereb Cortex. 2005; 15:708–719. [PubMed: 15371291]

44. Baiano M, David A, Versace A, Churchill R, Balestrieri M, Brambilla P. Anterior cingulate volumes in schizophrenia: a systematic review and a meta-analysis of MRI studies. Schizophr Res. 2007; 93:1–12. [PubMed: 17399954]

45. Koo MS, Levitt JJ, Salisbury DF, Nakamura M, Shenton ME, McCarley RW. A cross-sectional and longitudinal magnetic resonance imaging study of cingulate gyrus gray matter volume abnormalities in first-episode schizophrenia and first-episode affective psychosis. Arch Gen Psychiatry. 2008; 65:746–760. [PubMed: 18606948]

46. Kreczmanski P, Heinsen H, Mantua V, Woltersdorf F, Masson T, Ulfig N, Schmidt-Kastner R, Korr H, Steinbusch HW, Hof PR, Schmitz C. Volume, neuron density and total neuron number in five subcortical regions in schizophrenia. Brain. 2007; 130:678–692. [PubMed: 17303593]

47. Kreczmanski P, Schmidt-Kastner R, Heinsen H, Steinbusch HW, Hof PR, Schmitz C. Stereological studies of capillary length density in the frontal cortex of schizophrenics. Acta Neuropathol. 2005; 109:510–518. [PubMed: 15886994]

48. Casanova MF, de Zeeuw L, Switala A, Kreczmanski P, Korr H, Ulfig N, Heinsen H, Steinbusch HW, Schmitz C. Mean cell spacing abnormalities in the neocortex of patients with schizophrenia. Psychiatry Res. 2005; 133:1–12. [PubMed: 15698672]

49. DSM-IV-TR, Diagnostic and Statistical Manual of Mental Disorders. American Psychiatric Association; 2000.

50. ICD-10, International Statistical Classification of Diseases and Related Health Problems. 10th revision ed. World Health Organization; 2007.

51. Heinsen H, Heinsen YL. Serial thick, frozen, gallycyanin stained sections of human central nervous system. J Histotechnol. 1991; 14:167–173.

52. Heinsen H, Beckmann H, Heinsen YL, Gallyas F, Haas S, Scharff G. Laminar neuropathology in Alzheimer's disease by a modified Gallyas impregnation. Psychiatry Res. 1989; 29:463–465. [PubMed: 2481861]

53. Braak H, Braak E. Staging of Alzheimer's disease-related neurofibrillary changes. Neurobiol Aging. 1995; 16:271–278. discussion 8-84. [PubMed: 7566337]

54. Heinsen H, Arzberger T, Schmitz C. Celloidin mounting (embedding without infiltration) -a new, simple and reliable method for producing serial sections of high thickness through complete human brains and its application to stereological and immunohistochemical investigations. J Chem Neuroanat. 2000; 20:49–59. [PubMed: 11074343]

55. Heinsen H, Henn R, Eisenmenger W, Gotz M, Bohl J, Bethke B, Lockemann U, Puschel K. Quantitative investigations on the human entorhinal area: left-right asymmetry and age-related changes. Anat Embryol (Berl). 1994; 190:181–194. [PubMed: 7818090]

56. Schmitz C, Hof PR. Design-based stereology in neuroscience. Neuroscience. 2005; 130:813–831. [PubMed: 15652981]

57. Barbas H, Rempel-Clower N. Cortical structure predicts the pattern of corticocortical connections. Cereb Cortex. 1997; 7:635–646. [PubMed: 9373019]

58. Roberts GW, Colter N, Lofthouse R, Bogerts B, Zech M, Crow TJ. Gliosis in schizophrenia: a survey. Biol Psychiatry. 1986; 21:1043–1050. [PubMed: 2943323]

59. Sowell ER, Peterson BS, Thompson PM, Welcome SE, Henkenius AL, Toga AW. Mapping cortical change across the human life span. Nat Neurosci. 2003; 6:309–315. [PubMed: 12548289]

60. Selemon LD, Kleinman JE, Herman MM, Goldman-Rakic PS. Smaller frontal gray matter volume in postmortem schizophrenic brains. Am J Psychiatry. 2002; 159:1983–1991. [PubMed: 12450946]

61. Rimol LM, Hartberg CB, Nesvag R, Fennema-Notestine C, Hagler DJ Jr, Pung CJ, Jennings RG, Haukvik UK, Lange E, Nakstad PH, Melle I, Andreassen OA, Dale AM, Agartz I. Cortical thickness and subcortical volumes in schizophrenia and bipolar disorder. Biol Psychiatry. 2010; 68:41–50. [PubMed: 20609836]

62. Kikinis Z, Fallon JH, Niznikiewicz M, Nestor P, Davidson C, Bobrow L, Pelavin PE, Fischl B, Yendiki A, McCarley RW, Kikinis R, Kubicki M, Shenton ME. Gray matter volume reduction in rostral middle frontal gyrus in patients with chronic schizophrenia. Schizophr Res. 2010; 123:153–159. [PubMed: 20822884]

63. Pomarol-Clotet E, Canales-Rodriguez EJ, Salvador R, Sarro S, Gomar JJ, Vila F, Ortiz-Gil J, Iturria-Medina Y, Capdevila A, McKenna PJ. Medial prefrontal cortex pathology in schizophrenia as revealed by convergent findings from multimodal imaging. Mol Psychiatry. 2010; 15:823–830. [PubMed: 20065955]

64. Selemon LD, Goldman-Rakic PS. The reduced neuropil hypothesis: a circuit based model of schizophrenia. Biol Psychiatry. 1999; 45:17–25. [PubMed: 9894571]

65. Harrison PJ. The neuropathology of schizophrenia. A critical review of the data and their interpretation. Brain. 1999; 122:593–624. [PubMed: 10219775]

66. Bouras C, Kövari E, Hof PR, Riederer BM, Giannakopoulos P. Anterior cingulate cortex pathology in schizophrenia and bipolar disorder. Acta Neuropathol. 2001; 102:373–379. [PubMed: 11603813]

67. Pakkenberg B. Total nerve cell number in neocortex in chronic schizophrenics and controls estimated using optical disectors. Biol Psychiatry. 1993; 34:768–772. [PubMed: 8292680]

68. Thune JJ, Uylings HB, Pakkenberg B. No deficit in total number of neurons in the prefrontal cortex in schizophrenics. J Psychiatr Res. 2001; 35:15–21. [PubMed: 11287052]

69. Benes FM, McSparren J, Bird ED, SanGiovanni JP, Vincent SL. Deficits in small interneurons in prefrontal and cingulate cortices of schizophrenic and schizoaffective patients. Arch Gen Psychiatry. 1991; 48:996–1001. [PubMed: 1747023]

70. Benes FM, Davidson J, Bird ED. Quantitative cytoarchitectural studies of the cerebral cortex of schizophrenics. Arch Gen Psychiatry. 1986; 43:31–35. [PubMed: 3942472]

71. Rajkowska G, Selemon LD, Goldman-Rakic PS. Neuronal and glial somal size in the prefrontal cortex: a postmortem morphometric study of schizophrenia and Huntington disease. Arch Gen Psychiatry. 1998; 55:215–224. [PubMed: 9510215]

72. Chana G, Landau S, Beasley C, Everall IP, Cotter D. Two-dimensional assessment of cytoarchitecture in the anterior cingulate cortex in major depressive disorder, bipolar disorder, and schizophrenia: evidence for decreased neuronal somal size and increased neuronal density. Biol Psychiatry. 2003; 53:1086–1098. [PubMed: 12814860]

73. Benes FM. Emerging principles of altered neural circuitry in schizophrenia. Brain Res Rev. 2000; 31:251–269. [PubMed: 10719152]

74. Ongur D, Drevets WC, Price JL. Glial reduction in the subgenual prefrontal cortex in mood disorders. Proc Natl Acad Sci U S A. 1998; 95:13290–13295. [PubMed: 9789081]

75. Cotter D, Mackay D, Landau S, Kerwin R, Everall I. Reduced glial cell density and neuronal size in the anterior cingulate cortex in major depressive disorder. Arch Gen Psychiatry. 2001; 58:545–553. [PubMed: 11386983]

76. Selimbeyoglu A, Parvizi J. Electrical stimulation of the human brain: perceptual and behavioral phenomena reported in the old and new literature. Front Hum Neurosci. 2010; 4:46. [PubMed: 20577584]

77. Habel U, Chechko N, Pauly K, Koch K, Backes V, Seiferth N, Shah NJ, Stocker T, Schneider F, Kellermann T. Neural correlates of emotion recognition in schizophrenia. Schizophr Res. 2010; 122:113–123. [PubMed: 20663646]

78. Ghashghaei HT, Hilgetag CC, Barbas H. Sequence of information processing for emotions based on the anatomic dialogue between prefrontal cortex and amygdala. NeuroImage. 2007; 34:905–923. [PubMed: 17126037]

79. Davidson RJ, Pizzagalli D, Nitschke JB, Putnam K. Depression: perspectives from affective neuroscience. Annu Rev Psychol. 2002; 53:545–574. [PubMed: 11752496]

80. Konner, M. Universals of Behavioral Development in Relation to Brain Myelination. In: Gibson, KR.; Petersen, AC., editors. Brain Maturation and Cognitive Development. New York: Aldine de Gruyter; 1991. p. 181-223.

81. Marenco S, Weinberger DR. The neurodevelopmental hypothesis of schizophrenia: following a trail of evidence from cradle to grave. Dev Psychopathol. 2000; 12:501–527. [PubMed: 11014750]

82. Weinberger DR. Implications of normal brain development for the pathogenesis of schizophrenia. Arch Gen Psychiatry. 1987; 44:660–669. [PubMed: 3606332]

83. Insel TR. Rethinking schizophrenia. Nature. 2010; 468:187–193. [PubMed: 21068826]

84. Weinberger DR, Lipska BK. Cortical maldevelopment, anti-psychotic drugs, and schizophrenia: a search for common ground. Schizophr Res. 1995; 16:87–110. [PubMed: 7577773]

85. Skudlarski P, Jagannathan K, Anderson K, Stevens MC, Calhoun VD, Skudlarska BA, Pearlson G. Brain connectivity is not only lower but different in schizophrenia: a combined anatomical and functional approach. Biol Psychiatry. 2010; 68:61–69. [PubMed: 20497901]

86. Fallon JH, Opole IO, Potkin SG. The neuroanatomy of schizophrenia: circuitry and neurotransmittor systems. Clin Neurosci Res. 2003; 1-2:77–107.

87. Zalesky A, Fornito A, Seal ML, Cocchi L, Westin CF, Bullmore ET, Egan GF, Pantelis C. Disrupted axonal fiber connectivity in schizophrenia. Biol Psychiatry. 2011; 69:80–89. [PubMed: 21035793]

88. Kubicki M, Niznikiewicz M, Connor E, Nestor P, Bouix S, Dreusicke M, Kikinis R, McCarley R, Shenton M. Relationship Between White Matter Integrity, Attention, and Memory in Schizophrenia: A Diffusion Tensor Imaging Study. Brain Imaging Behav. 2009; 3:191–201. [PubMed: 20556231]

89. Whitford TJ, Kubicki M, Schneiderman JS, O'Donnell LJ, King R, Alvarado JL, Khan U, Markant D, Nestor PG, Niznikiewicz M, McCarley RW, Westin CF, Shenton ME. Corpus callosum abnormalities and their association with psychotic symptoms in patients with schizophrenia. Biol Psychiatry. 2010; 68:70–77. [PubMed: 20494336]

90. Takei K, Yamasue H, Abe O, Yamada H, Inoue H, Suga M, Muroi M, Sasaki H, Aoki S, Kasai K. Structural disruption of the dorsal cingulum bundle is associated with impaired Stroop performance in patients with schizophrenia. Schizophr Res. 2009; 114:119–127. [PubMed: 19505800]
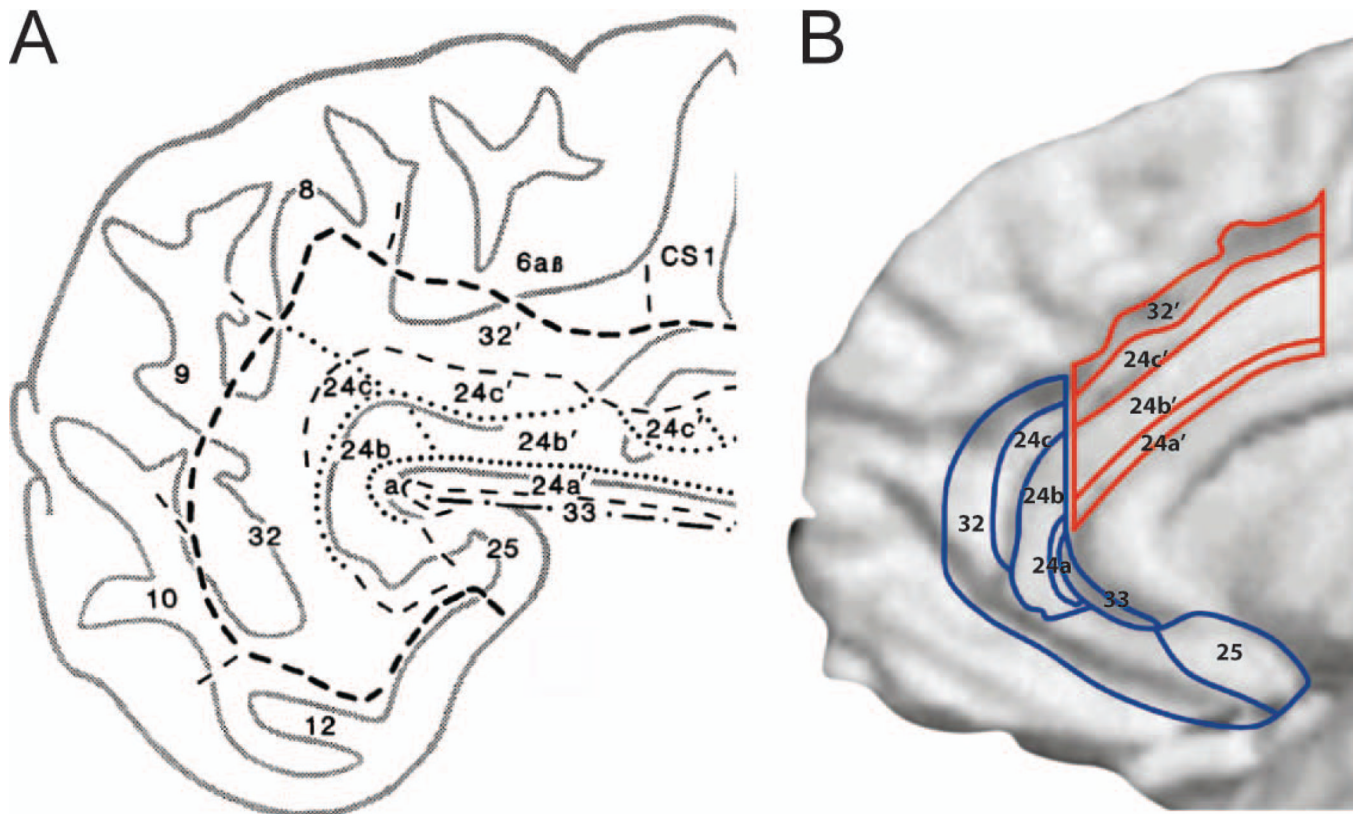
Figure 1.
(A) The anterior cingulate region (ACC) as delineated by Vogt, encompassing the rostral areas 24a-c and the dorsal areas 24a'-c', bordering the paracingulate area 32 and 32' and the subgenual area 25. Modified from [19]. (B) The rostral (blue/affective) and dorsal (red/cognitive) anterior cingulate regions depicted on a reconstructed MRI, of the medial surface of the right hemisphere of a human brain. Modified from [31].
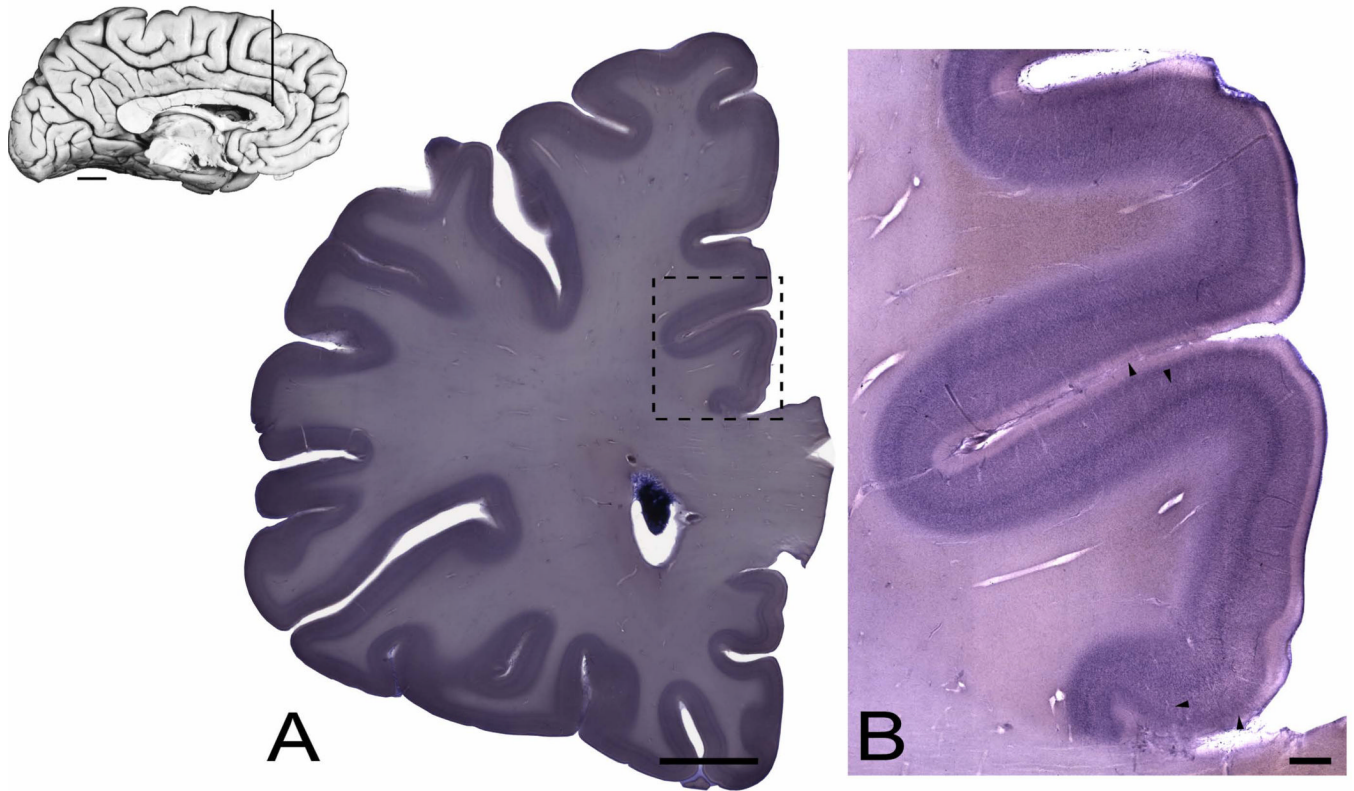
Figure 2.
Inset: A mid-sagittal photograph of the left hemisphere of a human brain showing the cingulate gyrus. The vertical line corresponds to a representative coronal section that contains the region of interest. Scale bar = 1 cm. (A) Gallocyanine-stained coronal section showing the localization of the investigated region, the dorsal anterior cingulate (dACC, within dashed box) in a control subject. Scale bars = 1 cm. (B) Photomontage of the dACC corresponding to areas 24a'-c', illustrating the cytoarchitectonic features at each level from a control subject. Arrowheads indicate borders among areas 33, 24a', 24b', 24c', and 32', respectively, moving dorsally from the corpus callosum. Scale bar = 1 mm.
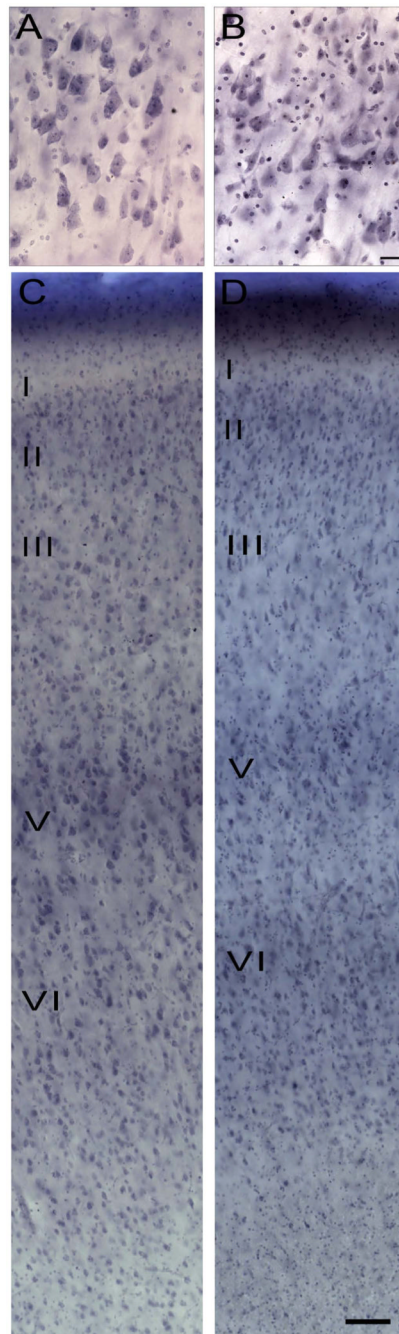
Figure 3.
Photomicrographs depicting typical cellular features in layer V of area 24b' in a control
subject (A) and in a patient with schizophrenia (B). Note the many satellite oligodendrocytes
surrounding pyramidal cell perikarya. Scale bar = 25 μm. Photomicrographs depicting the
six cortical layers in area 24b' in a control (C) and in a patient with schizophrenia (D). Scale
bar = 100 μm.
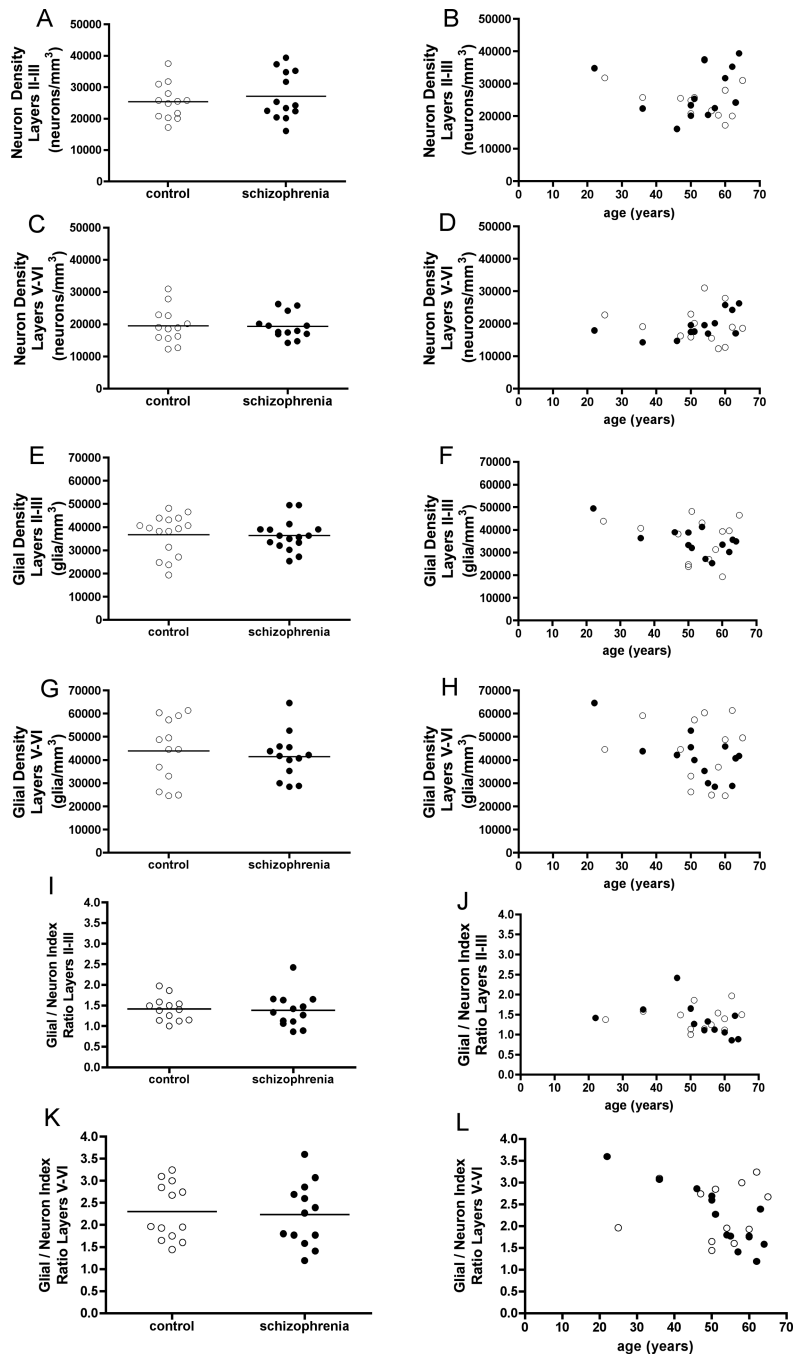
Figure 4.

Figure 4. (A-D) Variations in neurons in controls (open circles) and in patients with schizophrenia (filled circles), in superficial (II-III) and deep (V-VI) layers of the dACC volume (corresponding to area 24a'-c'). Estimated neuron densities between groups (A, C), and across age (B, D).

(E-H) Variations in glial cells (oligodendrocytes and astrocytes) in controls (open circles) and in patients with schizophrenia (filled circles), in superficial (II-III) and deep (V-VI) layers of the dACC volume (corresponding to area 24a'-c'). Estimated glial densities between groups (E, G), and across age (F, H).

(I-L) Variations in GNI ratios (glial density/neuron density) in controls (open circles) and in patients with schizophrenia (filled circles), in superficial (II-III) and deep (V-VI) layers of the dACC volume (corresponding to area 24a'-c'). GNI ratios between groups (I, K), and across age (J, L).

Table 1

Clinical characteristics of cases included in the present study.

Case #	Age at death	Age at onset	Illness duration	Adjusted illness duration*	Cause of death	PMI	Fix	Diagnosis	
	[years]	[years]	[years]	[years]		[hours]	[days]	DSM-IV	ICD-10
C1	25				Cardiac tamponade	14	119		
C2	36				Gunshot	24	143		
C3	47				Acute myocardial infarct	24	133		
C4	50				Acute myocardial infarct	35	433		
C5	50				Avalanche accident	23	498		
C6	51				Septicemia	7	285		
C7	54				Acute myocardial infarct	18	168		
C8	56				Acute myocardial infarct	60	3570		
C9	58				Acute myocardial infarct	28	126		
C10	60				Gastrointestinal hemorrhage	18	101		
C11	60				Gastrointestinal hemorrhage	27	302		
C12	62				Acute myocardial infarct	24	3696		
C13	65				Bronchopneumonia	6	2289		
S1	22	19	3	26	Suicide‡	88	130	295.30	F20.00
S2	36	28	8	31	Suicide‡	<72	115	295.30	F20.00
S3	46	24	22	45	Systemic hypothermia	<24	327	295.30	F20.01
S4	50	17	33	56	Peritonitis	<24	203	295.30	F20.00
S5	50	22	28	51	Suicide	18	170	295.30	F20.00
S6	51	17	34	57	Septicemia	33	127	295.60	F20.50
S7	54	20	34	57	Septicemia	27	250	295.60	F20.50
S8	55	22	33	56	Right-sided heart failure	25	84	295.30	F20.00
S9	57	37	20	43	Septicemia	76	163	295.30	F20.00
S10	60	24	36	59	Pulmonary embolism	<48	311	295.30	F20.01
S11	62	19	43	66	Aspiration	7	171	295.30	F20.00
S12	63	22	41	64	Acute myocardial infarct	15	338	295.60	F20.50
S13	64	26	38	61	Pulmonary embolism	6	817	295.60	F20.50

Case #	Age at death [years]	Age at onset [years]	Illness duration [years]	Adjusted illness duration* [years]	Cause of death	PMI [hours]	Fix [days]	Diagnosis	
								DSM-IV	ICD-10
Mean C	51.9 ± 3.1					24 ± 4	247 ± 53		
Mean S	51.5 ± 3.3	22.9 ± 1.5				27 ± 6	912 ± 372		

C - control; S - schizophrenia;

*
Adjusted illness duration, see Materials and Methods.

‡
Case S1 and S2 had long post-mortem intervals, however they were both found within 1h of death and were kept at 4°C until autopsy.

DSM-IV: Diagnostic and Statistical Manual of Mental Disorders, 4th Edition [49].

ICD-10: International Statistical Classification of Diseases and Related Health Problems [50].

Table 2

Details of the stereological parameters.

Section periodicity	6
Section z-intervals (μm)	4200
Objective 1	2.5x
Objective 2	40x
Guard zone (μm)	5
Counting frame (μm)	75×75
Grid (μm)	1250×1250
Disector height (μm)	25
Disector volume (μm³)	140 625